The Penetration and Movement of Nanoparticles on Membrane

Lianxin Xin^a, Zixuan Wang^a, Jian Zhao^a, Zachary Tyler ^a, Hacene Boukari ^a, Essaid Zerrad ^a, and Jun Ren^{a*}

^aDelaware State Univ., 1200 Dupont Hwy., Dover, DE USA 19901

ABSTRACT

In this study, we used GROMACS, a versatile package for performing molecular dynamics to simulate the interactions between different nanoparticles and Dipalmitoyl PhosPhatidyl Choline (DPPC) to understand the physical mechanisms that govern the interactions between nanoparticles and lipid membrane. Our simulations show the responses of the lipid bilayer to the nanoparticles, including the formation of an adsorbent layer on the nanoparticle surface, transmembrane ectopic movements and inconspicuous endocytosis of the nanoparticle by the membrane. Effects of the size of the nanoparticles, structural shape and charge state on the interaction and transport processes will be examined and summarized.

Keywords: Gold Nanoparticles, DPPC, Cell Membrane, GROMACS, Molecular Dynamics

1. INTRODUCTION

Over the past decade nanomedicine has emerged rapidly, bringing the capabilities of combining nanotechnology with biological sciences [1-3]. Furthermore, with the fast advancement of computation techniques, interactions of nanomaterials with cells can now be more precisely simulated and visualized, renovating the prospective of site-specific and target-acute goal in drug delivery through nano engineering and nanoscience studies [4-6].

It is of great importance to study the detailed dynamic processes during the interactions of nanomaterials with cell membranes and other biological systems, since nanomaterials may also introduce damages and alterations to untargeted biological systems [7, 8]. In this study, our simulations focus on the interactions of gold nanoparticles (AuNP) with DPPC membrane. We applied the DPPC model membrane system in our study to help us understand different development of interactions between AuNP and the DPPC membrane including infiltration, endocytosis-like wrapping and adsorption, etc. Effects of AuNP size and shape, and external factors including concentration of cations and anions in the solvent will also be investigated.

Studies have been carried out on dynamic simulations of nanoparticles (NP) interacting with lipid bilayers [9-11], where the translocation capability and the influences on the lipid bilayers are compared between hydrophilic NP and hydrophobic NP. Neutral NPs are found to be less efficient in forming defects on the bilayer surface and hence enhancing NP penetration through the membrane. In our study, we used neutral AuNP as target and concentrate on morphology alterations of the lipid bilayer by AuNP, including formation of adsorption layers on nanoparticle surfaces and decreases of orders in the lipid hydrophobic cores.

With the great potentials of nanomaterials in carrying and transporting drugs to targeted cells and tissues in a defined and well-regulated way, knowledge and systematic understandings of the interaction processes between nanoparticles and tissue membranes are essential. Particularly the cytotoxicity impacts introduced by nanoparticles and nanostructures have to be characterized and carefully categorized into lasting and recoverable groups. Our results will be valuable in designing the optimal nanostructures to treat disease cells without introducing toxicity and disruptions to normal cells.

^{*}jren@desu.edu; phone 1 302 857-6809; fax 1 302 857-7482; desu.edu

2. METHODS

2.1 Force Field

In our GROMACS [12-14] simulations, we chose GROMOS96 53A6 [15, 16] as the simulation force field. GROMOS force field is targeted at solving molecular system with high precision over a long period of time, where the non-bond interactions are described by the Lenard-Jones interaction function and the electrostatic interactions by the Coulomb function,

$$V_{LJ} = \sum \left(\frac{c_{12ij}}{r_{ij}^{12}} - \frac{c_{6ij}}{r_{ij}^{6}}\right)$$
 (Eq.-1)

$$V_e = \frac{q_i q_j}{4\pi\varepsilon_0 \varepsilon_r r_{ij}} \tag{Eq.-2}$$

Molecule's initial coordinates are arranged on a cubic periodic grid; bad contacts between molecules are removed by steepest descent minimization; and molecule initial velocities are defined by the Maxwell-Boltzmann distribution at 298K. System is equilibrated using the conjugate gradient method to optimize the minimum energy, followed by another round of equilibration at constant pressure [17].

2.2 DPPC Membrane and AuNP

We use 128DPPC model membrane in our study to simulate the interactions between AuNP and the lipid membrane. Our DPPC membrane is about 4.1nm in thickness. Applying model membrane allows experimental verifications and comparisons to be carried out under standard conditions and hence is highly repeatable. Our DPPC structure is obtained from the University of Calgary Biocomputing group website [18].

AuNPs with diameters of 1nm, 2nm and 3nm are generated using the Nanoparticle Builder Module in the Open source Molecular Dynamic engine (OpenMD) [19]. The positions of the gold atoms in the AuNP are determined by the AuNP size using the gold lattice constant of 0.408nm.

Figure 1 shows an illustration of the DPPC system with Au nanoparticles of 1nm, 2nm and 3nm sizes placed on the top and on the bottom of the bilayer surface, respectively, as the initial configuration. The coordinates of each molecule in this initial configuration are then extracted using OpenMD, and the data are used as an input file for the subsequent AuNP and lipid bilayers interaction simulation.

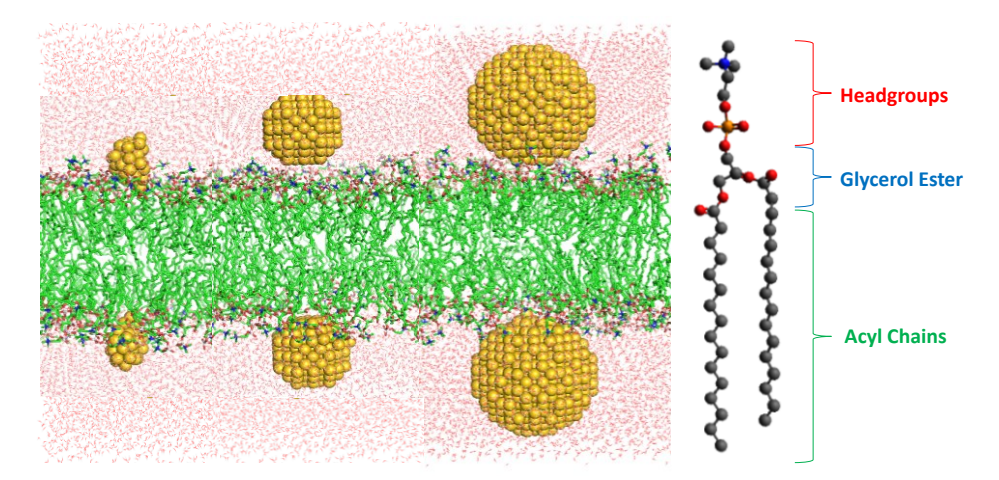


Figure 1. An illustration of the Dipalmitoyl PhosPhatidyl Choline (DPPC) system with Au nanoparticles (AuNPs). DPPC is used in this study as a lipid bilayer structure to interact with AuNPs of 1nm, 2nm and 3nm in size, from left to right, respectively.

2.3 Simulations

Our simulations are implemented using GROMACS simulation package, version 2018 [13], which are embedded with minimal communication domain decomposition algorithms, parallel constraint solvers, and parallel molecular simulation implementation. Particle mesh Ewald (PME) algorithms [20] for long range electrostatics and linear constraint solver (LINCS) [21] are also incorporated in the algorithm.

Our system consists of 128DPPC molecules surrounded by \sim 6700 to 12900 water molecules, with 0-3 AuNPs and 0-80 Cl ions. A 6.4nm×6.4nm × (8.6-12.6) nm box with a periodic boundary condition is set up for the simulation. Our simulations run for time interval over 10-100 ns with a step size of 2 fs.

Three types of interactions are observed between AuNP and DPPC, i.e. AuNP interacts with the headgroups of lipids; with the hydrophobic acyl chains; and with both the headgroups and the acyl chains.

3. RESULTS

3.1 Formation of the Adsorption Layers on AuNP Surfaces

For neutral AuNP, interactions of the nanoparticle with DPPC headgroups and the lipid tails are governed by the van der Waals force. Figure 2 shows formation of adsorption layers on AuNP surfaces, with the adsorption layer mostly made by the lipid tails shown in Fig. 2a and the enlarged layer region shown in Fig. 2c. Figure 2b shows the adsorption layer formed by DPPC head groups followed by the lipid tails. The layer region is expanded and shown in Fig. 2d. The AuNP size in Fig. 2 is 2nm and the total simulation time interval is 10ns. Attachment of the DPPC headgroups and the lipid tails to the surface of AuNP indicates alterations of the lipid membrane structures.

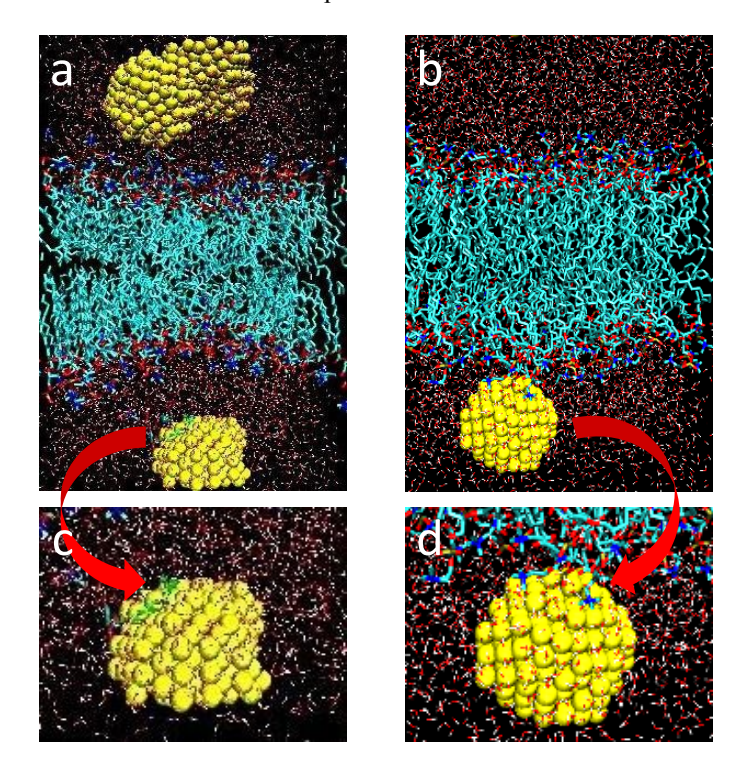


Figure 2. Formation of the adsorption layers on AuNP surfaces: (a) mostly by the DPPC lipid tails; and (b) by the DPPC headgroups followed by the lipid tails. The enlarged snapshots of the adsorption layers of (a) and (b) are shown in (c) and (d), respectively. The AuNP size is 2nm and the total time interval is 10ns.

Since van der Waals interaction is relatively weak, in Fig. 2 the distribution of the adsorption layers on the nanoparticle surface is random and the interaction is not strong enough to move the AuNP inside the DPPC bilayers. Alternatively, if

nanoparticle surface is coated with hydrophilic and hydrophobic ligands, it has been found that the nanoparticles would be readily adsorbed into the lipid bilayers [22].

3.2 AuNP Moves across the DPPC Membrane

Nanoparticle size is an important factor in determining the possibility of nanoparticle transmembrane movement. A threshold radius has been reported, below which particles are incapable of entering and crossing the membrane. The threshold radius and the optimal radius vary depending on nanoparticle's type, shape, surface area, surface charge and hydrophobicity and hydrophobicity states, etc. [23, 24].

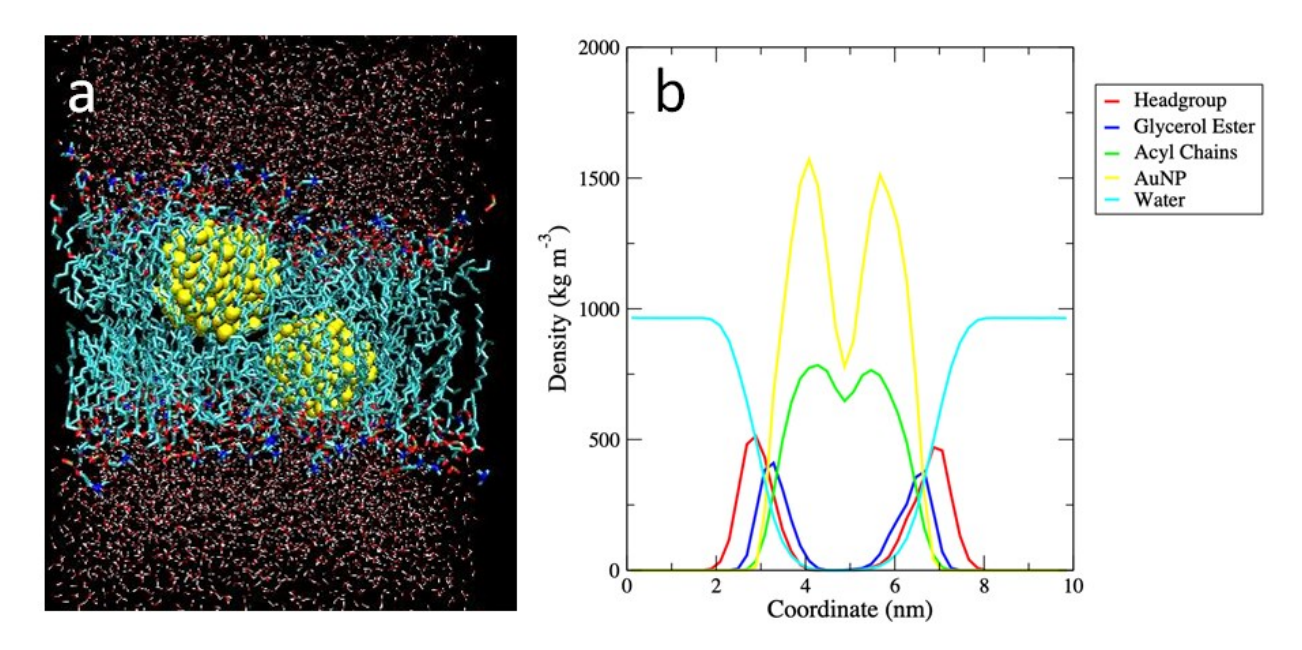


Figure 3. Movements of AuNP across DPPC membrane: (a) AuNP with r = 1nm ectopically moving through the DPPC hydrophilic head groups and making incisions in the hydrophobic core; (b) partial density plot showing a full overlap between AuNPs and the hydrophobic DPPC Acyl chains. The total time interval is 100ns.

In our study, we tested neutral AuNP with sizes of 1nm, 2nm and 3nm, respectively. We find that AuNP of 2nm makes the best DPPC membrane entry. Figure 3 illustrates the movements of two AuNPs with r = 1nm across the DPPC membrane. The AuNPs were initially aligned horizontally and placed on the top and on the bottom of the DPPC bilayer surfaces. A snapshot of the AuNPs and the DPPC membrane at t = 100ns is shown in Fig. 3a, where the two AuNPs are found to penetrate completely into the membrane with slight shifts from their original horizontal positions. Partial density plot of the two AuNPs and the DPPC membrane is shown in Fig. 3b, where a complete overlap can be found between the AuNPs and the DPPC hydrophobic Acyl chains.

3.3 Endocytosis-like Wrapping of AuNP by DPPC

Nanoparticles may pass through a cell membrane by direct diffusion and endocytosis-like wrapping movement. Larger spherical nanoparticles were found to undertake endocytosis-like wrapping more likely than smaller nanoparticles. Furthermore, strong interactions with the membrane headgroups may also increase chances of endocytosis-like wrapping. Hence the movement possibly is the result of lower free energy generated from the combined effects of adhesion energy at the surface and bending energy from membrane deformation [25-27].

Our simulations also show that when AuNP size increases to 3nm, endocytosis-like wrapping occurs between AuNP and DPPC. Figure 4 illustrates the snapshot at t = 100ns of an AuNP (the bottom one) inconspicuously wrapped by the DPPC headgroups and the carbon tails. In Fig. 4a, the two AuNPs shown were initially aligned horizontally and placed on the top and on the bottom of the DPPC bilayer surfaces. At t = 100ns, the bottom AuNP is partially wrapped around by the DPPC headgroups and the hydrophobic Acyl chains. Partial density plot of the two AuNPs and the DPPC membrane is shown in Fig. 4b, where a full overlap between the bottom AuNP and the DPPC headgroup and a partial

overlap between the bottom AuNP and Acyl chains confirm the endocytosis-like wrapping interactions. From Fig4a and Fig4b, no disruptions and noticeable alterations of the DPPC membrane structure by the AuNP insertion can be observed.

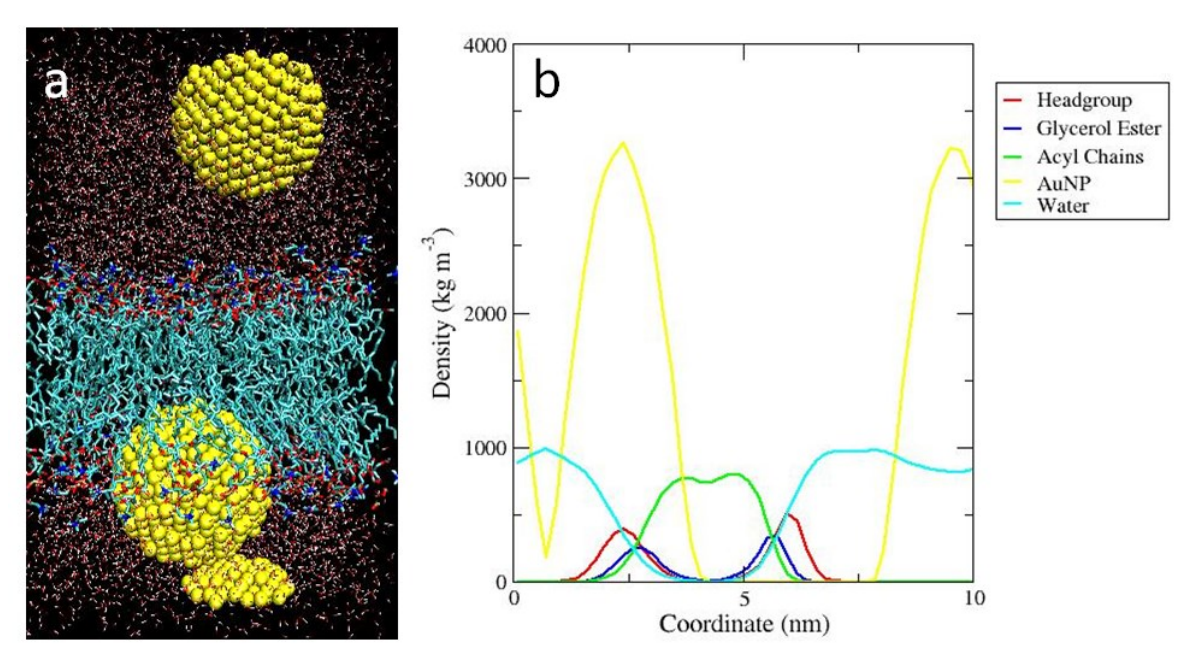


Figure 4. AuNP inconspicuously endocytosed by the DPPC headgroups and the carbon tails: (a) wrapping of DPPC around AuNP, AuNP r = 1.5nm; (b) partial density plot showing a full overlap with the headgroup and a partial overlap with the Acyl chains. The total time interval is 100ns.

3.4 AuNP Aggregation

When small size nanoparticles are placed close to each other or in high concentrations, nanoparticle aggregation would take place because the van der Waals forces are stronger and hence the nanoparticle attractions are larger. Figure 5 shows the aggregation of AuNPs and its impact on nanoparticle transmembrane movements. Figure 5a shows that at t = 0ns, three AuNPs with r = 1nm were placed near the DPPC bilayer surfaces, two on the top and one at the bottom. Figure 5b shows that at t = 10ns, the top two AuNPs are attached to each other and formed a cluster.

When compared with Figure 3, we notice that the newly formed cluster is trapped near the membrane surface instead of making movement toward and across the lipid membrane. Interestingly, it also affects the transmembrane movement of the AuNP at the other side of the membrane. The bottom AuNP is stranded on the membrane surface and starts to form an adsorption layer at its surface by extracting the hydrophobic Acyl chains from the membrane. Studies on the nanoparticle aggregation have shown that NP aggregation makes translocation across the cell membrane more difficult [28, 29]. Nonetheless, to our knowledge, it is the first report that NP aggregation could negatively affect the movement of nanoparticles on the opposite side of the lipid membrane.

3.5 AuNP with sizes of 1nm, 2nm and 3nm

To further study the impact of the AuNP size on the nanoparticle movement across and on the DPPC lipid membrane, the transport and membrane penetration behaviors for AuNP with sizes of 1nm, 2nm and 3nm are studied and compared. Figure 6 shows the comparisons of DPPC interacting with AuNPs of different sizes. At t = 0ns, snapshots of two AuNPs (on the top and on the bottom of the DPPC bilayer surface) with sizes of 1nm, 2nm and 3nm are shown in Fig. 6a, Fig. 6b and Fig. 6c, respectively. The impacts of the AuNP sizes on the transportation and penetration behaviors at t = 100ns are shown in Fig. 6d, Fig. 6e and Fig. 6f, correspondingly.

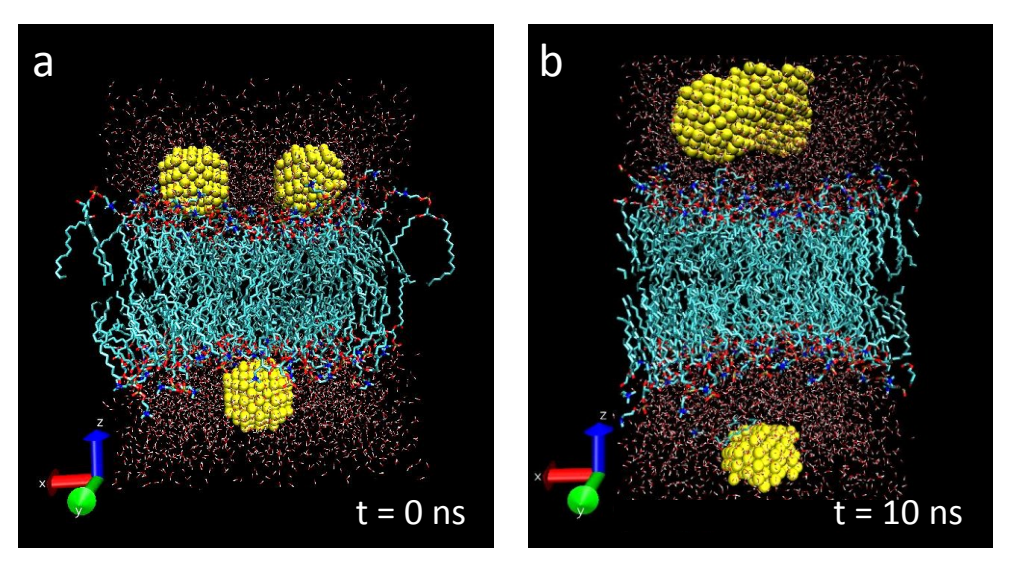


Figure 5. Three AuNPs with sizes of 2nm were placed on the top (with two AuNPs) and at the bottom (with one AuNP) of DPPC. The small AuNP sizes and the close spacing between neighboring nanoparticles (NPs) enhance NP agrregation; (a) at t = 0ns; (b) at t = 10ns. The aggregation of two AuNPs at the top of DPPC shifts the NP movements to further away from the DPPC surfaces.

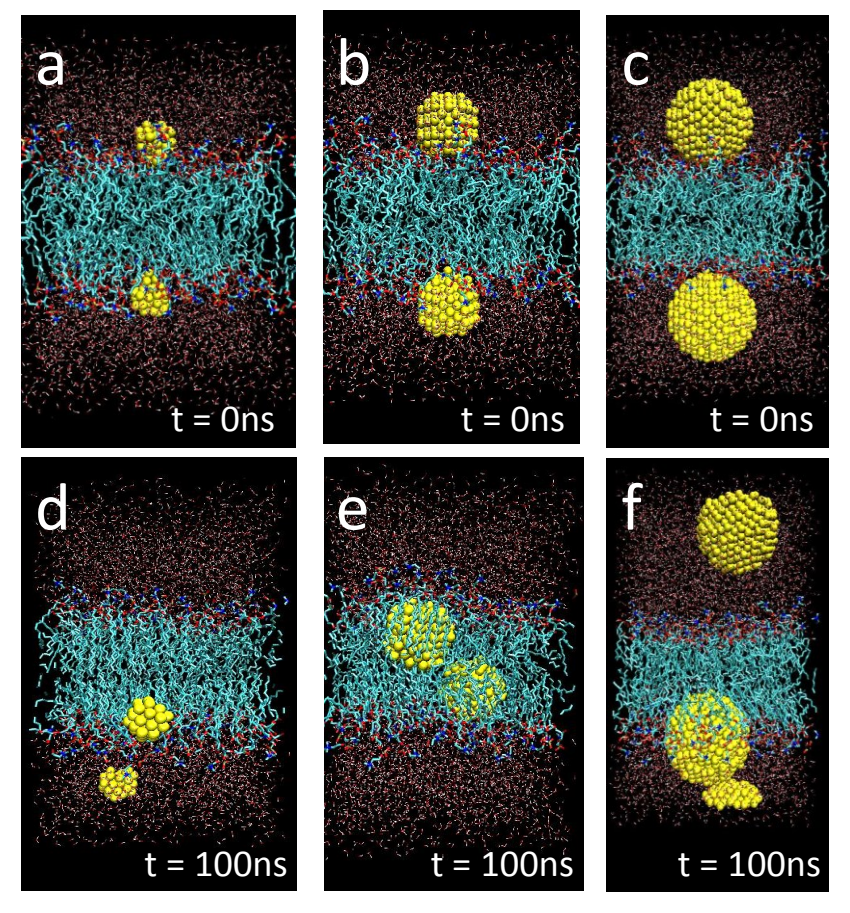


Figure 6. Comparisons of DPPC interacting with AuNPs of different sizes. At t = 0ns, the sizes of the nanoparticles are (a) r = 0.5nm; (b) r = 1nm and (c) r = 1.5nm, respectively. The impacts of the AuNP sizes on the interactions with DPPC memebrane at t = 100ns are shown in (d), (e)and (f) correspondingly.

For AuNP of 1nm size, the gold nanoparticles are unable to cross the DPPC membrane; for AuNP of 2nm size, the NPs penetrate completely into the DPPC membrane with slight horizontal shifts; and for AuNP of 3nm size, the DPPC membrane wraps around the AuNP. Note in Fig. 8a and Fig. 8d, the top AuNP takes an upward movement away from the membrane. Because our simulation box holds a periodic boundary, when the top AuNP hits the upper boundary, it will reappear from bottom of the simulation box.

To compare the influences of the AuNP sizes on the DPPC membrane structure, we carry out the Deuterium order parameter (Scd) analysis. Scd is the order parameter defined by the angle of the carbon-deuterium bond (C-D bond),

$$S_{cd} = <\frac{3\cos^2\alpha - 1}{2}>$$
 (Eq.-3)
Here α is the angle between the C-D bond and the z-axis. [30-32].

Figure 7 shows that when DPPC membrane interacts with AuNPs, the DPPC structure characterized by the Deuterium order parameter changes. Dependence of the Deuterium order parameter on AuNP sizes of (a) r = 0 (no AuNP, only the DPPC); (b) r = 0.5nm; (c) r = 1nm; and (d) r = 1.5nm are shown in Fig. 7a, Fig. 7b, Fig. 7c and Fig. 7d, respectively. The Deuterium order parameters signifying the orders of the DPPC carbon chains (sn1 chain and sn2 chain) increase initially with small AuNP of r = 0.5nm (the DPPC lipid hydrophobic cores become more ordered and dense) but decrease rapidly when AuNP size r = 1.5nm (the DPPC lipid hydrophobic cores become less ordered and more loose). Here the sn2 chain is connected to the middle carbon of the glycerol backbone and is therefore on average positioned slightly closer to the membrane surface than the sn1 chain.

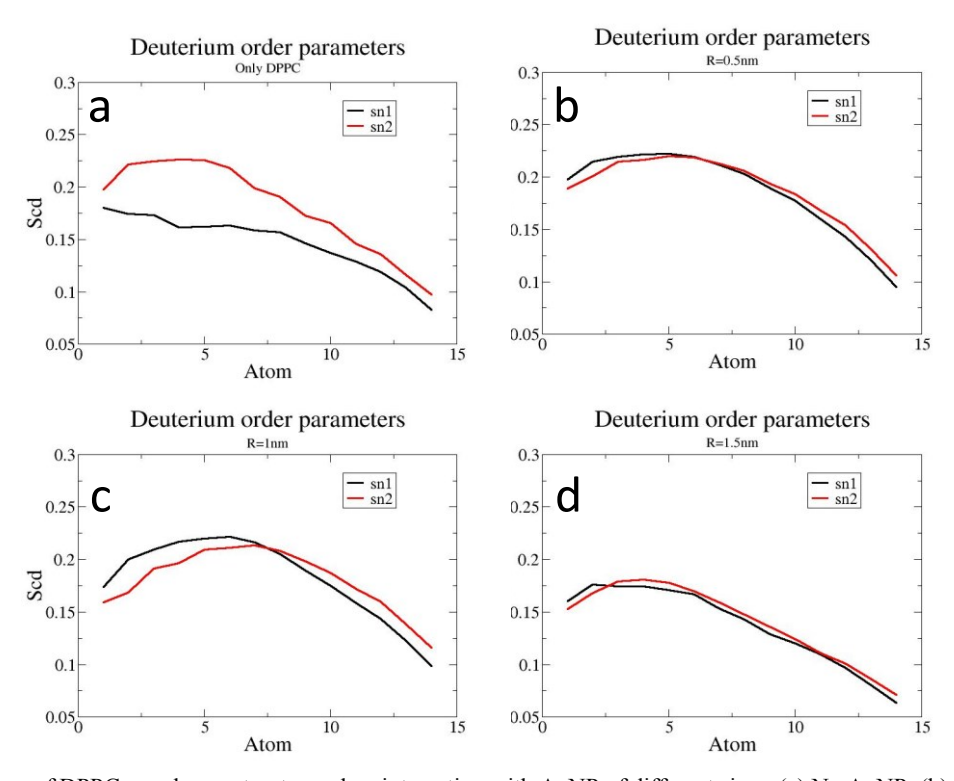


Figure 7. Changes of DPPC membrane structure when interacting with AuNP of different sizes. (a) No AuNP; (b) AuNP r = 0.5nm; (c) AuNP r = 1nm; and (d) AuNP r = 1.5nm. The Deuterium order parameters representing the orders of the DPPC carbon chains (sn1 and sn2) increase initially with small AuNP but decrease rapidly when AuNP size r = 1.5nm.

3.6 Cl anions in the solvent

To study the transportation and penetration behaviors of AuNP through DPPC membrane in an ionic environment, we add Cl anions to the system. Cl is a hydrophilic anion and hence has less effects on the DPPC headgroups. Figure 8 shows the interactions of DPPC with r = 1nm AuNPs in different ionic environments. At t = 0ns, snapshots of two AuNPs (on the top and on the bottom of the DPPC bilayer surface) in the ionic environments with different number of added Cl⁻ ions of (a) 0; (b) 20 and (c) 80 are shown in Fig. 8a, Fig. 8b and Fig. 8c, respectively. The impacts of the added Cl⁻ ions on the AuNP and DPPC interaction at t = 10ns are shown in Fig. 8d, Fig. 8e and Fig. 8f, correspondingly.

Comparing Fig. 8e with Fig. 8d, we notice that when the amount of added Cl⁻ ions = 20, AuNP is incapable of making contacts with the DPPC membrane (because our simulation box holds a periodic boundary, when the bottom AuNP moving away from the membrane hits the lower boundary, it will reappear from top of the simulation box). When the amount of added Cl⁻ ions = 80, the transportation and penetration behavior of AuNP in Fig. 8f show no improvements, if not worse, comparing to Fig. 8d.

Deuterium order parameter analysis is carried out in Figure 9, where the number of added Cl⁻ ions in Fig. 9a, Fig. 9b and Fig. 9c are 0, 20 and 80, respectively. Figure 9 shows that the orders of the DPPC carbon chains (sn1 and sn2) decrease rapidly with more Cl⁻ ions. The deterioration of the orders in DPPC lipid hydrophobic cores is very likely introduced by the bonding of the hydrophilic anions Cl⁻ with the DPPC hydrophobic Acyl chains, hence bringing damages and alterations to the DPPC structure.

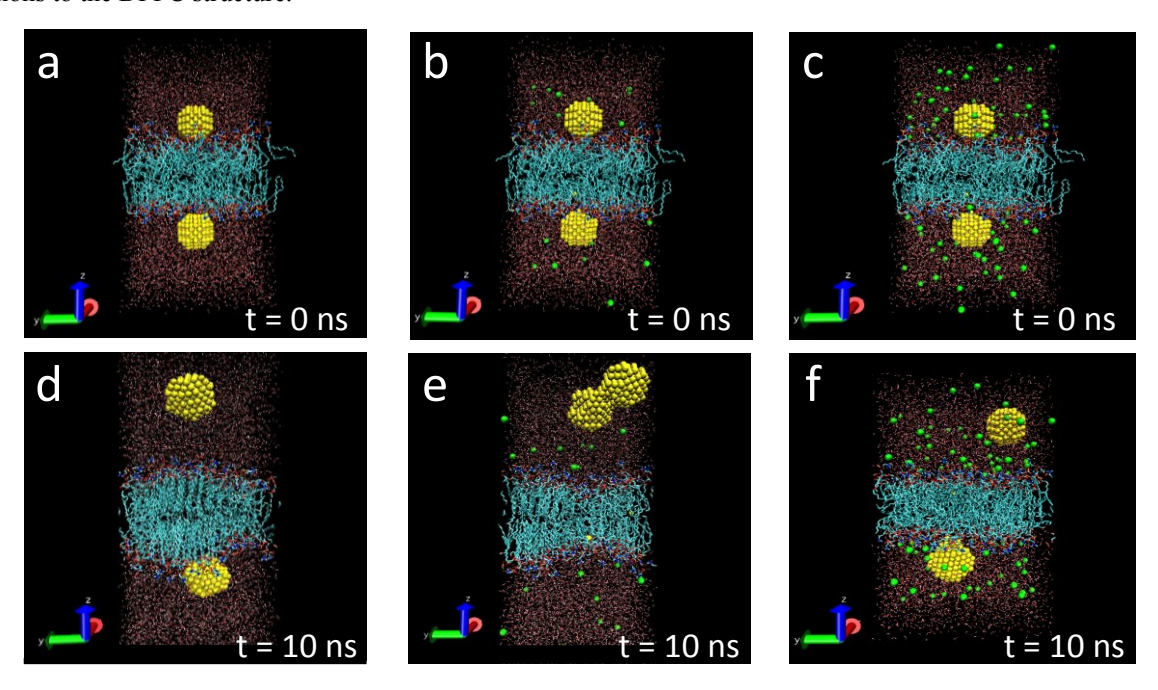


Figure 8. Interaction of DPPC with r = 1nm AuNPs in different solvent environment. At t = 0ns, the number of added Cl⁻ ions are (a)0; (b) 20 and (c) 80, respectively. The impacts of the added ions at t = 10ns are shown in (d), (e) and (f) correspondingly.

4. DISCUSSION

In this study, we used DPPC as a model membrane to mimic the natural bilayer lipid membrane bordering between the cytoplasm and the extracellular environment, as well as between the cell's organelles and their intracellular cytoplasm [33, 34]. The transportation of nanoparticles as drug carriers through cell membrane could be of two directions, i.e. into the cell and out of the cell.

In our simulations, we placed AuNPs at the top and at the bottom of DPPC membranes to explore the characteristics and the relations between the two transportation processes. Using this simplified membrane model system, we find that the AuNPs placed on top of the DPPC membrane are prone to move away from the lipid surface, whereas the AuNPs placed on the bottom move toward and into the membrane. One possible explanation is that the top NPs imitates nanoparticles outside the cell that has larger momentum and more random moving directions imparted by the open fluid environment. The bottom NPs, on the other hand, are more constrained inside the cell and hence the influences of the van der Waals forces from the headgroups and the hydrophobic acyl chains are more evident.

Further simulations will be carried out to collect details of the interaction processes and establish better understandings.

5. SUMMARY

In summary, our simulations show the interaction processes between gold nanoparticles (AuNPs) and the DPPC lipids bilayers. including formation of adsorbent layer on the nanoparticle surface, transmembrane ectopic movements of the nanoparticles and inconspicuous endocytosis-like wrapping by the membrane. In the meantime, the presence of the gold nanoparticles also causes changes of the DPPC structure, i.e. the orders of the DPPC carbon chains (sn1 and sn2) increase with small AuNPs but drop rapidly when AuNPs size r=1.5nm. Adding ions to the solvent environment also reduces the orders of the DPPC carbon chains.

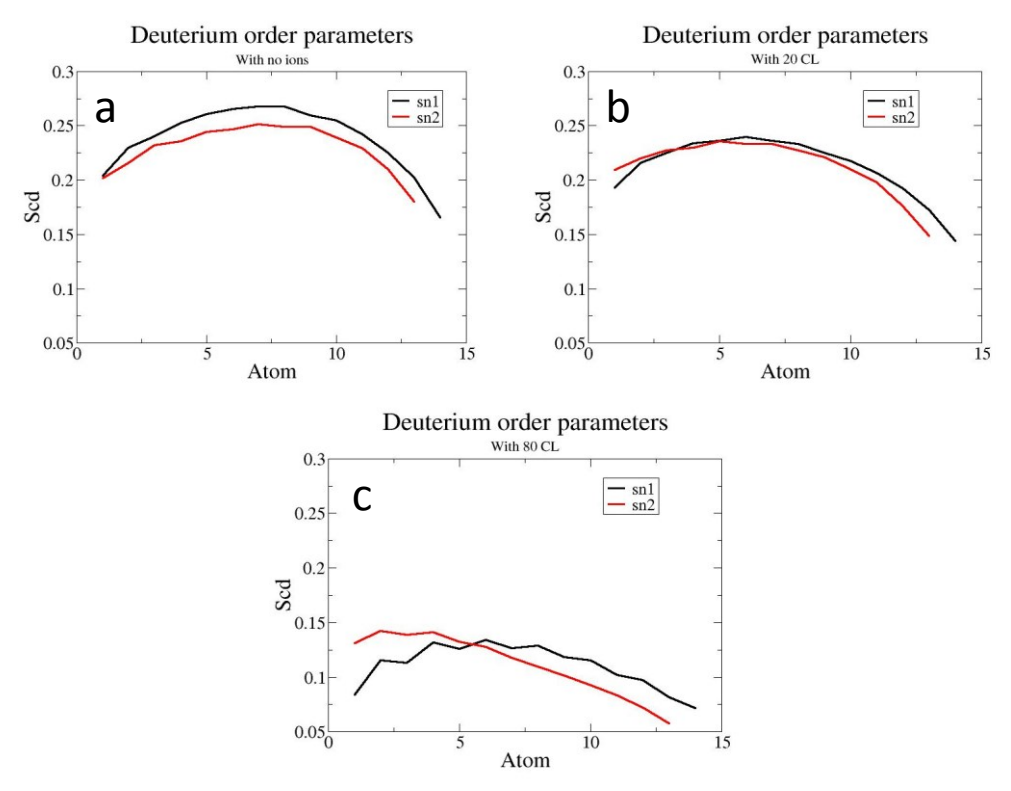


Figure 9. Changes of DPPC membrane structure with more Cl⁻ ions added to the solvent environment. (a) No ions; (b) 20 ions; and (c) 80 ions. The orders of the DPPC carbon chains (sn1 and sn2) decrease with the increase of added Cl⁻ ions.

REFERENCE

- [1] Jahangirian, H., G.Lemraski, E., Webster, T. J., Rafiee-Moghaddam, R., and Abdollahi, Y., "A review of drug delivery systems based on nanotechnology and green chemistry: green nanomedicine," Int J Nanomed. 12, 2957-2978 (2017)
- [2] Zhang, L., Gu, F.X., Chan, J. M., Wang, A. Z., Langer, R. S., and Farokhzad, O. C., "Nanoparticles in medicine: Therapeutic applications and developments, Clinical Pharmacology & Therapeutics," 83, 761-769 (2008)
- [3] Ramosl, A. P., Cruzl, M. A. E., Tovanil, C. B., and Ciancaglinil, P., "Biomedical applications of nanotechnology," Biophys Rev, 9, 79-89 (2017)
- [4] Behzadi, S., Serpooshan, V., Tao, W., et al. "Cellular uptake of nanoparticles: journey inside the cell," Chem Soc Rev. 46, 4218-4244 (2017)
- [5] Murphy, C. J., Vartanian, A. M., Geiger, F. M., et al. "Biological Responses to Engineered Nanomaterials: Needs for the Next Decade," ACS Central Science, 1, 117-123 (2015)
- [6] Ding, H. M., and Ma, Y. Q., "Theoretical and Computational Investigations of Nanoparticle-Biomembrane Interactions in Cellular Delivery," SMALL, 11, 1055-1071 (2015)
- [7] Lin, J., Zhang, H., Chen, Z., and Zheng, Y., "Penetration of lipid membranes by gold nanoparticles: insights into cellular uptake, cytotoxicity, and their relationship," ACS nano, 4, 5421-5429 (2010)

- [8] Ding, H. M., Tian, W. D., and Ma, Y. Q., "Designing Nanoparticle Translocation through Membranes by Computer Simulations," ACS nano, 6, 1230-1238 (2012)
- [9] Zolghadr, A. R., and Moosavi, S. S, "Interactions of neutral gold nanoparticles with DPPC and POPC lipid bilayers: simulation and experiment," RSC Advances, 9, 5197-5205 (2019)
- [10] Lin, X., Bai, Zuo, T. Y. Y., and Gu, N., "Promote potential applications of nanoparticles as respiratory drug carrier: insights from molecular dynamics simulations," NANOSCALE 6, 2759-2767 (2014)
- [11] Guzman, E., and Santini, E., "Lung surfactant-particles at fluid interfaces for toxicity assessments," Curr. Opin. Colloid Interface Sci, 39, 24-39 (2019)
- [12] Abraham, M.J., van der Spoel, D., Lindahl, E., Hess, B. and the GROMACS development team, "GROMACS User Manual version 2018," www.gromacs.org (2018)
- [13] Berendsen, H. J. C., van der Spoel, D., and van Drunen, R., "GROMACS: A message-passing parallel molecular dynamics implementation," Comp. Phys. Comm. 91:43–56 (1995)
- [14] Lindahl, E., Hess, B., and van der Spoel, D., "GROMACS 3.0: A package for molecular simulation and trajectory analysis," J. Mol. Mod. 7:306–317 (2001)
- [15] Scott, W. R. P., Hunenberger, P. H., Tironi, I. G, et al. "The GROMOS biomolecular simulation program package," J. Phys. Chem. A, 103, 3596-3607 (1999)
- [16] Oostenbrink, C., Villa, A., Mark, A. E., and Gunsteren, W. F. V., "A Biomolecular Force Field Based on the Free Enthalpy of Hydration and Solvation: The GROMOS Force-Field Parameter Sets 53A5 and 53A6," J Comput Chem, 25, 1656–1676 (2004)
- [17] Energy Minimization Methods, http://manual.gromacs.org/2019/reference-manual/algorithms/energy-minimization. html
- [18] Biocomputing Group using computer simulations to study biological problems, http://wcm.ucalgary.ca/tieleman/downloads
- [19] Gezelter, J., Kuang, S., Marr, J., et al., "OpenMD, an open source engine for molecular dynamics," University of Notre Dame, Notre Dame, IN (2010)
- [20] Essmann, U., Perera, L. Berkowitz, M. L., Darden, T., Lee, H., and Pedersen, L. G., "A Smooth Particle Mesh Ewald Method," J. Chem. Phys., 103, 8577-8593 (1995)
- [21] Hess, B., Bekker, H., Berendsen, H. J. C., and Fraaije, J. G. E.M., "LINCS: A linear constraint solver for molecular simulations," J. Comput. Chem, 18, 1463-1472 (1997)
- [22] Basak, U. K., Roobala, C., Basu, J. K., and Maiti, P. K., "Size-dependent interaction of hydrophilic/ hydrophobic ligand functionalized cationic and anionic nanoparticles with lipid bilayers," J. Condens. Matter Phys., 32, 104003 (2020)
- [23] Nel, A.E., Madler, L., Velegol, D., et al., "Understanding biophysicochemical interactions at the nano-bio interface," Nat. Mater., 8, 543-557 (2009)
- [24] Curtis, E. M., Bahrami, A. H., Weikl, T. R., and Hall, C. K., "Modeling nanoparticle wrapping or translocation in bilayer membranes," NANOSCALE, 7, 14505-14514 (2015)
- [25] Thake, T. H. F., Webb, J. R., Nash, A., Rappoport, J. Z., and Notman, R., "Permeation of polystyrene nanoparticles across model lipid bilayer membranes", Soft Matter, 9, 10265-10274 (2013)
- [26] Li, Y., Chen, X. and Gu, N., "Computational Investigation of Interaction between Nanoparticles and Membranes: Hydrophobic/Hydrophilic Effect," J. Phys. Chem., 112, 16647-16653 (2008)
- [27] Vacha, R., Martinez-Veracoechea, F. J., and Frenkel, D., "Receptor-Mediated Endocytosis of Nanoparticles of Various Shapes," Nano Lett., 11, 5391-5395 (2011)
- [28] Li, Y., Zhang, X. R., and Cao, D. P., "A spontaneous penetration mechanism of patterned nanoparticles across a biomembrane," Soft Matter, 10, 6844-6856 (2014)
- [29] Yue, K., Tang, J., Tan, H. Z., Lv, X. X., and Zhang, X. X., "Nanoparticle Aggregation in Ionic Solutions and Its Effect on Nanoparticle Translocation Across the Cell Membrane," J HEAT TRANS-T ASME, 11, 5391-5395 (2018)
- [30] Douliez, J. P., Leonard, A., and Dufourc, E. J., "Restatement of order parameter in biomembranes calculation of C-C bond order parameter from C-D quardupolar splittings," Biophys. J., 68, 1727-1739 (1995)
- [31] Klauda, J. B., Brooks, B. R., MacKerell, A. D., Venable, R. M. and Pastor, R. W., "An ab initio study on the torsional surface of alkanes and its effect on molecular simulations of alkanes and a DPPC bilayer," J. Phys. Chem. B, 109, 5300-5311 (2005)
- [32] Deuterium order parameter: One leaflet structure of DPPC lipid bilayer membrane, http://www.mdtutorials.com/gmx/membrane protein/09 analysis.html

- [33] Peetla, C., Stine, A., and Labhasetwar, V., "Biophysical Interactions with Model Lipid Membranes: Applications in Drug Discovery and Drug Delivery," Mol. Pharm., 6, 1264-1276 (2009)
 [34] Escriba, P. V., "Membrane-lipid therapy: a new approach in molecular medicine," Trends Mol. Med., 12, 34-
- 43 (2006)